Electronic Supplementary Material (ESI) for Biomaterials Science.

Granular Polyrotaxane Microgels As Injectable Hydrogels for Corneal Tissue Regeneration

Antonio J. Feliciano[1a], *Yousra Alaoui Selsouli*[1b], *Pamela Habibovic*[1b], *Zeinab Niloofar Tahmasebi Birgani*[1a,b], *Lorenzo Moroni*[1a], *Matthew B. Baker*[1a]
1 Maastricht University, MERLN Institute for Technology-Inspired Regenerative Medicine,
a Department of Complex Tissue Regeneration, Maastricht, Netherlands
b Department of Instructive Biomaterial Engineering

Supplementary Information

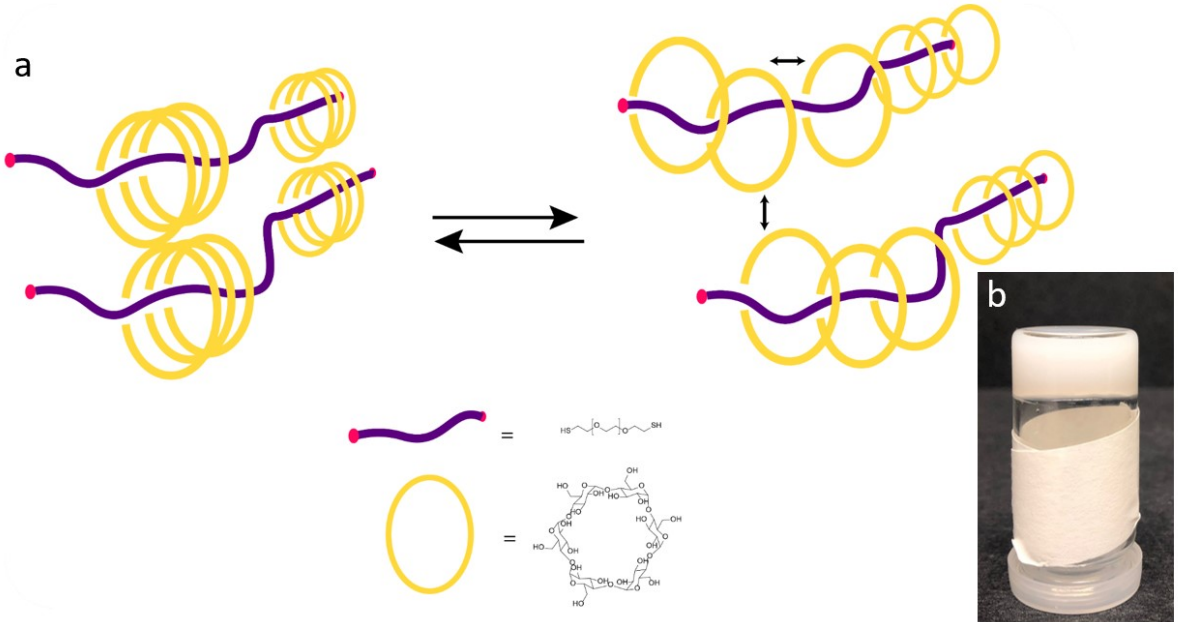

Figure S1. (a) schematic to produce polypseudorotaxane with αCD and PEGdithiol. (b) Inverted vial (5 mL) of 10% wt/v αCD with PEGdithiol showing supramolecular hydrogel formation.

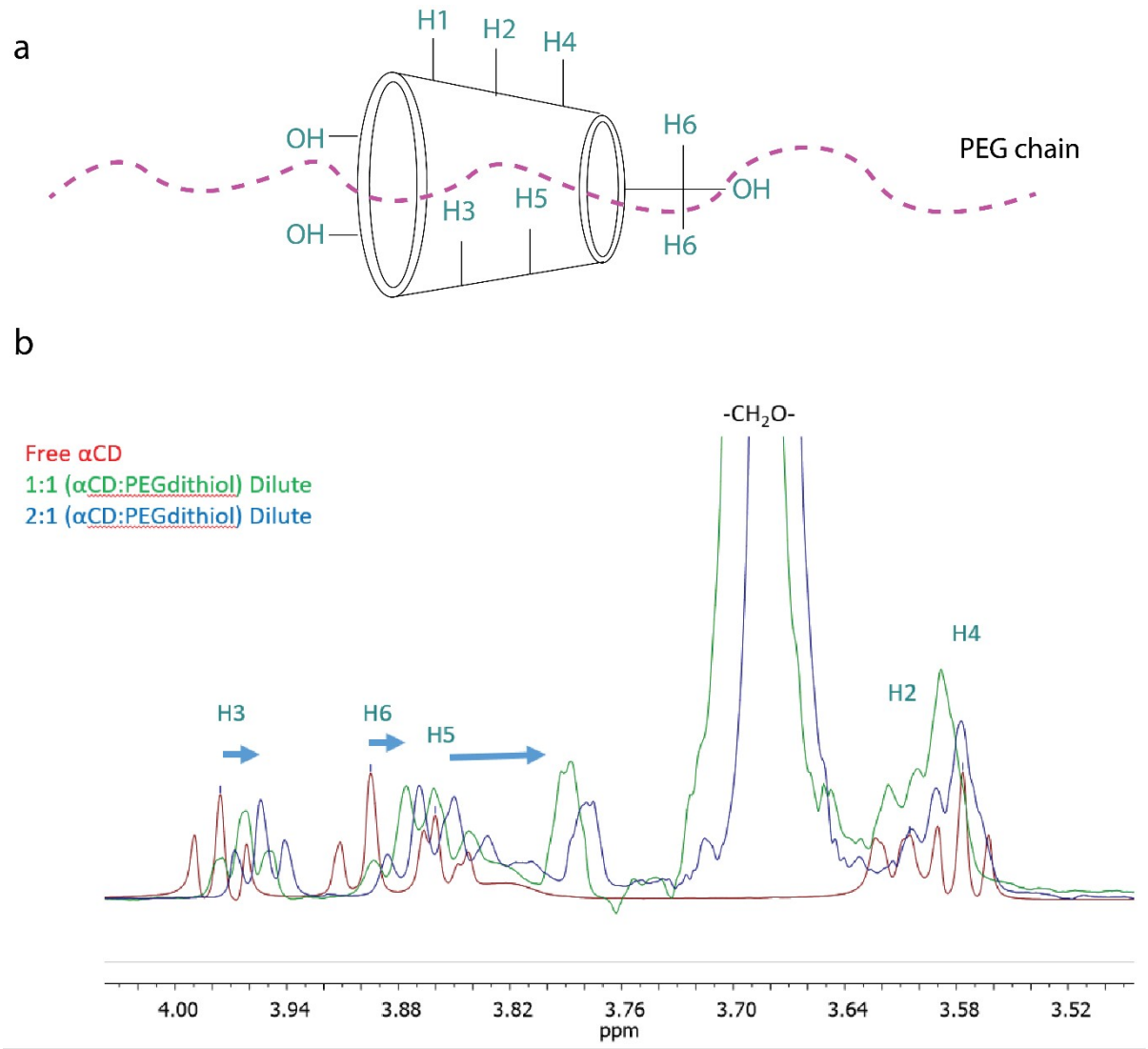

Figure S2. (a) Diagram of inclusion between CD macrocyle and PEG chain. (b) chemical shifts of αCD and PEG in 1:1 and 2:1 (αCD:PEG) ratios.

Table S1. Chemical shifts of protons indicating shifts between H3 and H5 protons indicating inclusion of PEG chain in CD.

		H1	H3	H6	H5	H2	H4
Ratio (αCD:PEG)	**Free αCD**	5.040	3.976	3.894	3.860	3.614	3.577
1:1	**Complex**	5.038	3.962	3.876	3.790	3.615	3.588
	Δδ	-0.002	-0.014	-0.018	-0.070	0.001	0.011
2:1	**Complex**	5.027	3.954	3.869	3.775	3.604	3.577
	Δδ	-0.013	-0.022	-0.025	-0.085	-0.01	0

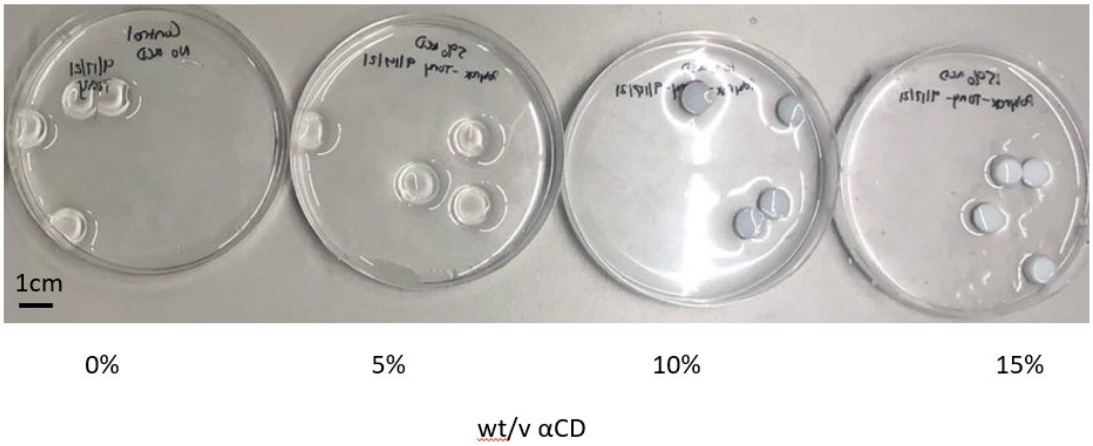

Figure S3. Synthesized bulk hydrogels after 2 days in PBS.

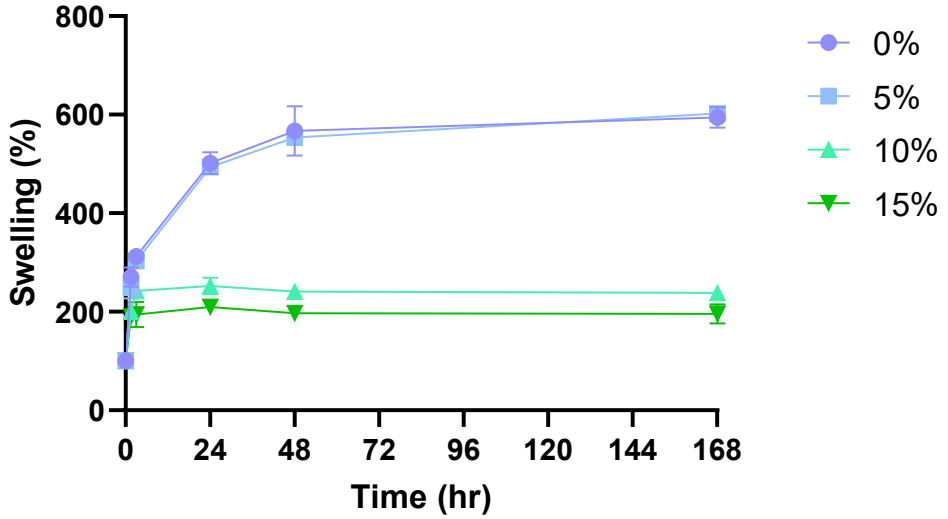

Figure S4. Swelling occurs the most with 0% αCD due to PEG chains being completely free to swell. 15% αCD has limited swelling due to secondary crosslinking between CDs.

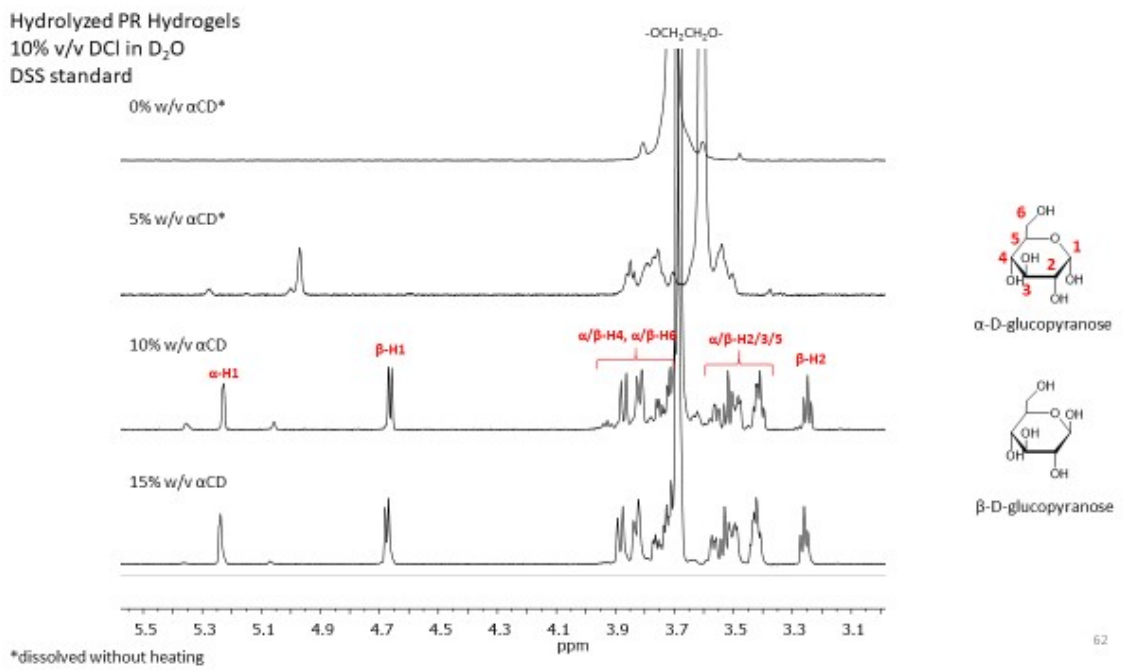

Figure S5. ^{1}H NMR of degradaded polyrotaxane hydrogel to determine the ratio of αCD to PEG in the final hydrogel.

Table S2. Calculated αCDs per PEGdithiol.

Sample	αCD-H1 integration	PEG integration	CD/PEG
0	0	-	NA
5	1	66,7	6
10	1,67	27,9	23
15	1,65	13,2	47

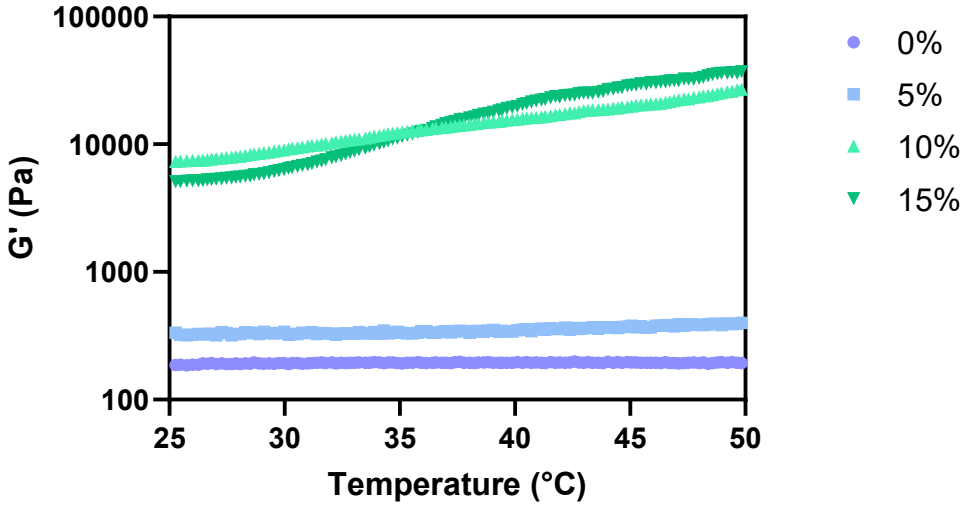

Figure S6. Thermoresponsiveness of bulk polyrotaxane gels. 10 and 15% wt/v αCD show clear increase in G' with increasing T whereas 0, 5% are negligible. Rate of temperature increase: 1ºC/min.

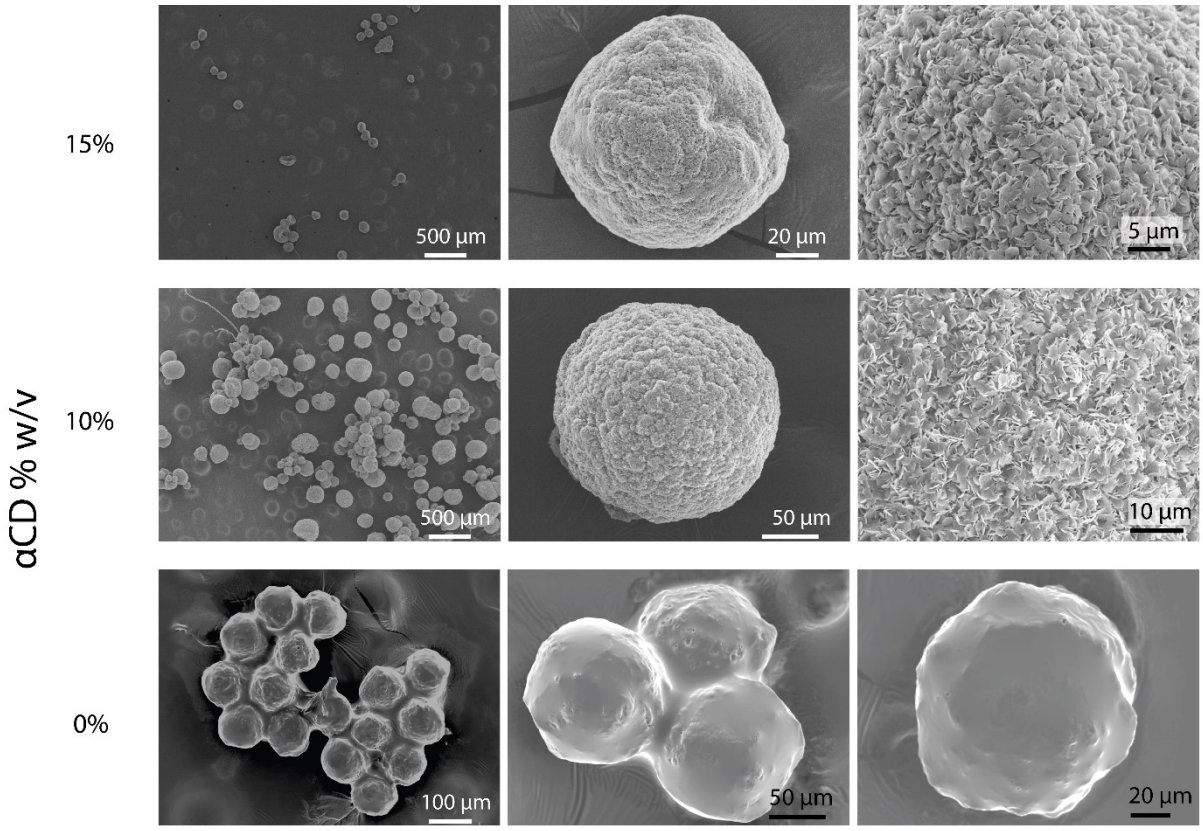

Figure S7. SEM images of 0, 10, 15% wt/v αCD GPR microgels after purification.

a

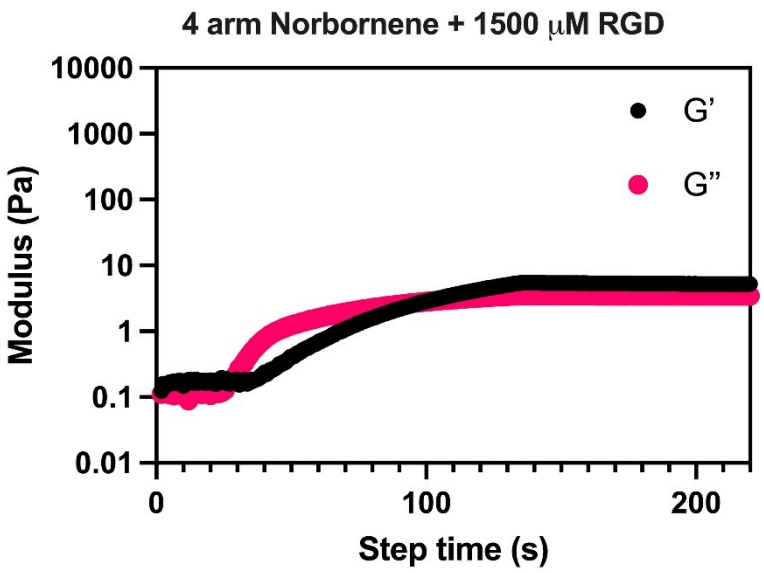
4 arm Norbornene + 1500 μM RGD
Modulus (Pa)
10000
1000
100
10
1
0.1
0.01
0
100
200
Step time (s)
G'
G"

b

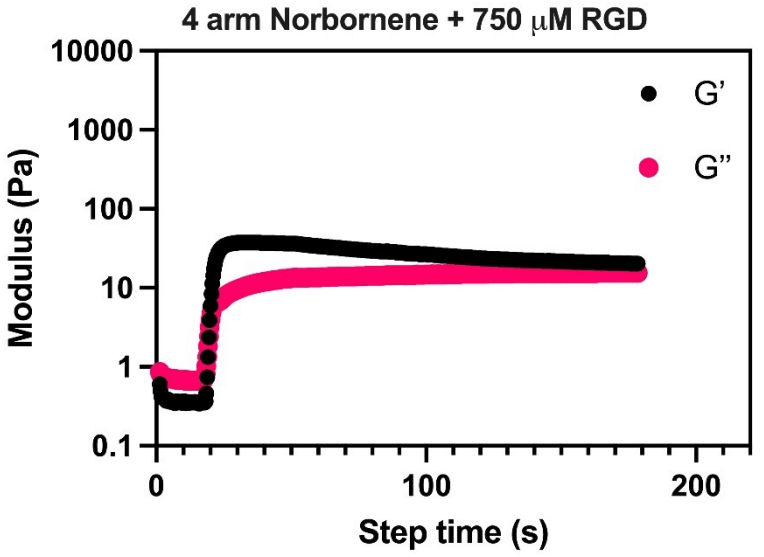
4 arm Norbornene + 750 μM RGD
Modulus (Pa)
10000
1000
100
10
1
0.1
0
100
200
Step time (s)
G'
G"

c

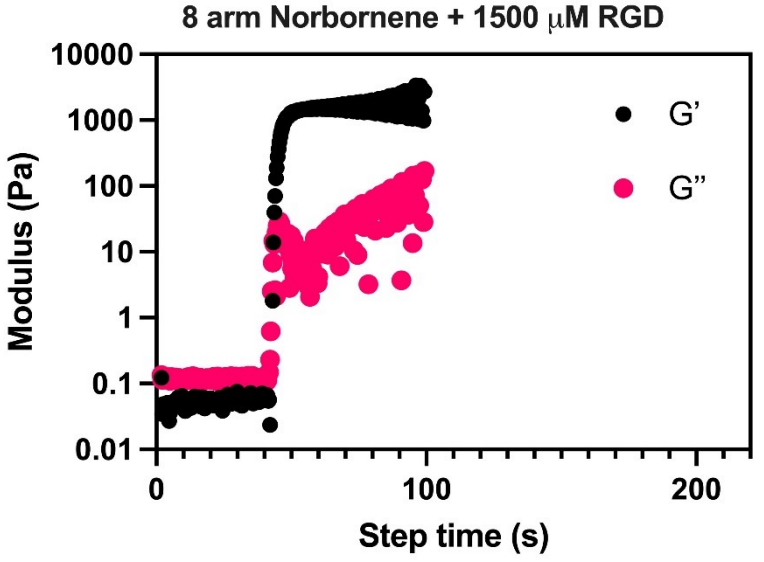
8 arm Norbornene + 1500 μM RGD
Modulus (Pa)
10000
1000
100
10
1
0.1
0.01
0
100
200
Step time (s)
G'
G"

Figure S8. Hydrogel gelation kinetics for different formulations of (15% wt/v αCD) polyrotaxane bulk hydrogels with (a) 4 arm norbornene (1.64 mM) and RGD (1500 μM) (b) 4 arm norbornene (1.5 mM) and RGD (750 μM) and (c) 8 arm norbornene (0.273 mM) and RGD (1500 μM) in MilliQ with 2 mM LAP. The concentration of thiol to norbornene functional groups was kept at 1:1.

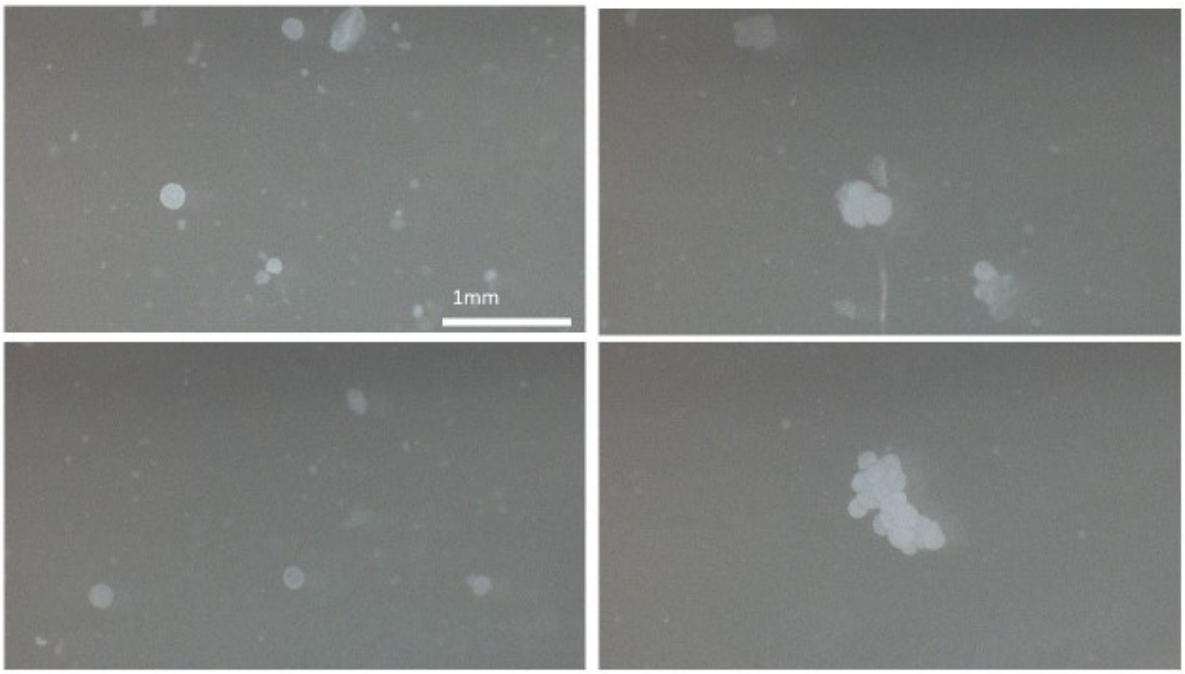

Figure S9. 8 arm RGD GPR microgels in water.

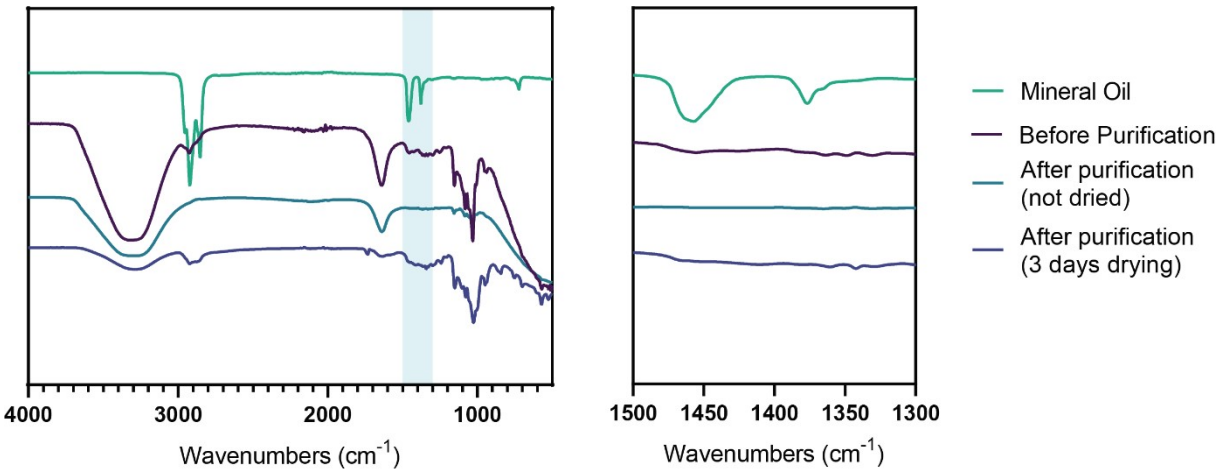

Figure S10. FTIR of purified GPR showcasing oil removal from GPR after synthesis. Residual oil removed after purification.

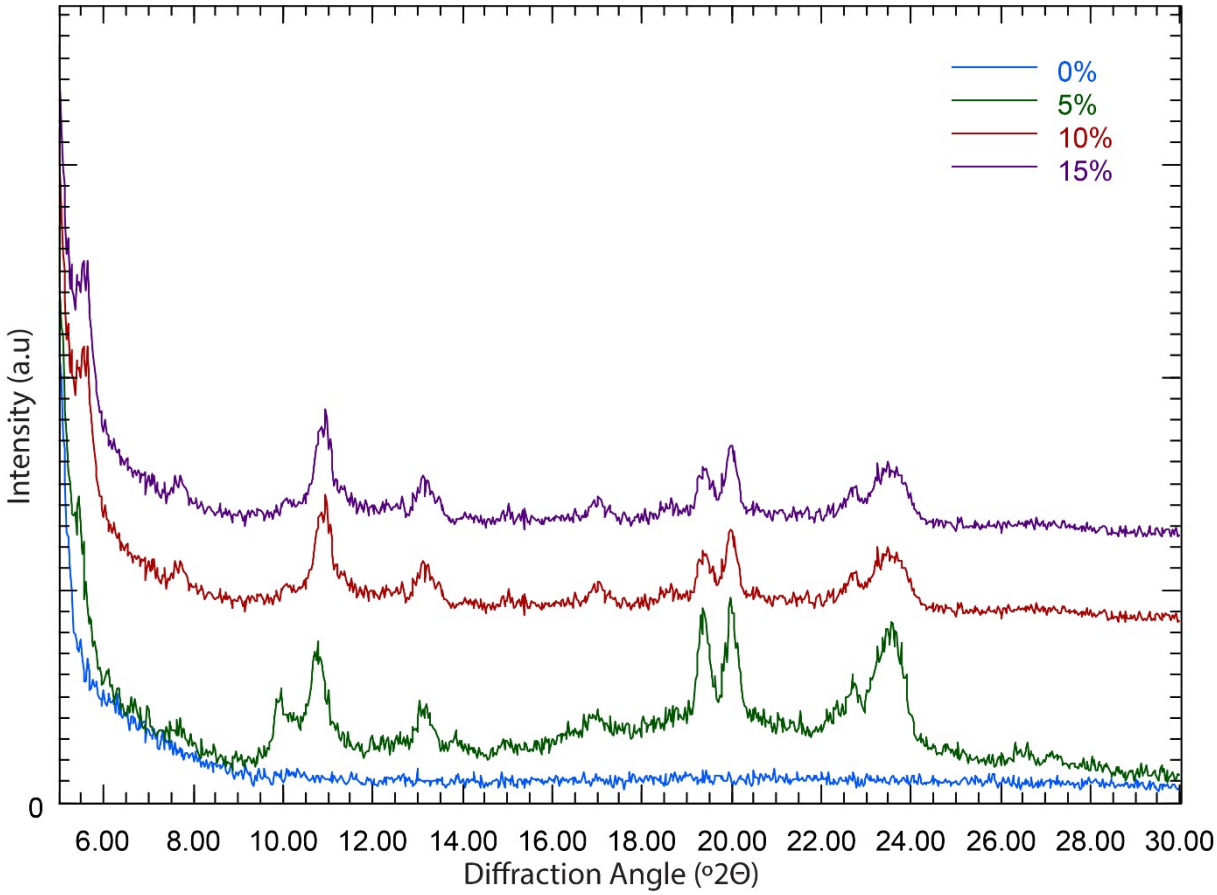

Figure S11. XRD of GPR dried microgels. No diffraction patterns observed for PEG microgels (0% αCD). Diffraction patterns appear with addition of 5 – 15% αCD.

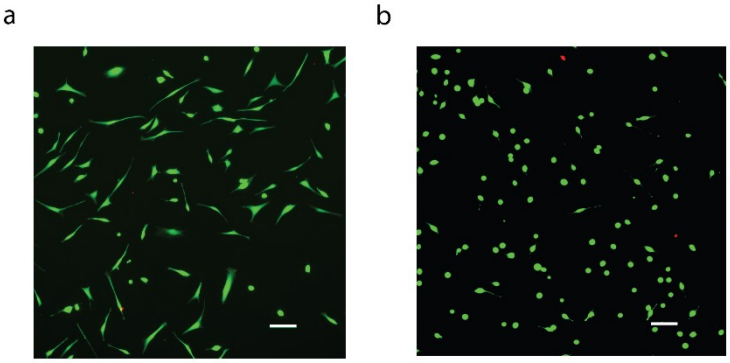

Figure S12. (a) Live/dead images of corneal keratocytes in differentiation media. (b) Morphological changes in human corneal keratocytes after 24 hours exposed to GPR supernatant. Scale bar = 100 μm.

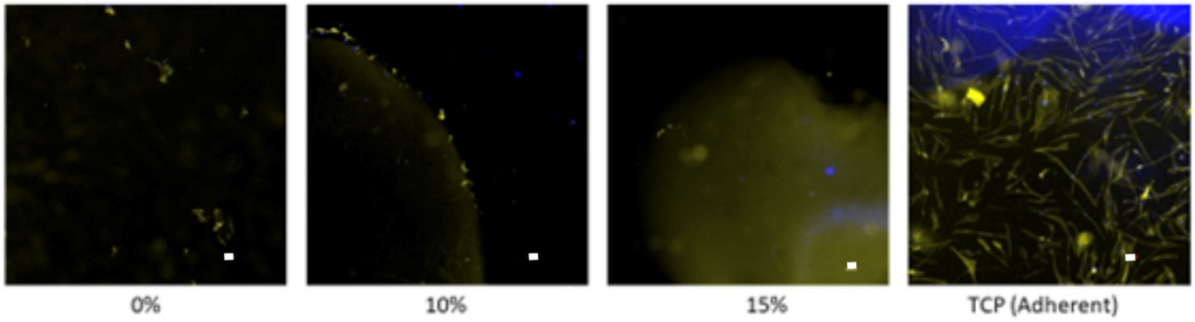

Figure S13. Bulk PR hydrogels after 2 weeks in culture with immortalized human corneal keratocytes indicating little to no adherence of cells to the bulk gel. Scale bar = 100 μm.

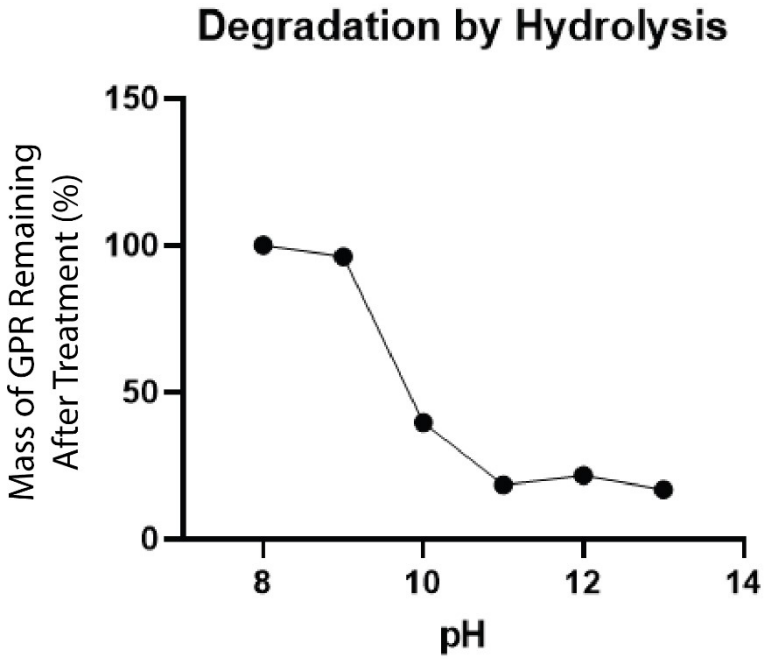

Figure S14. Degradability of GPR through basic hydrolysis monitored by mass loss.

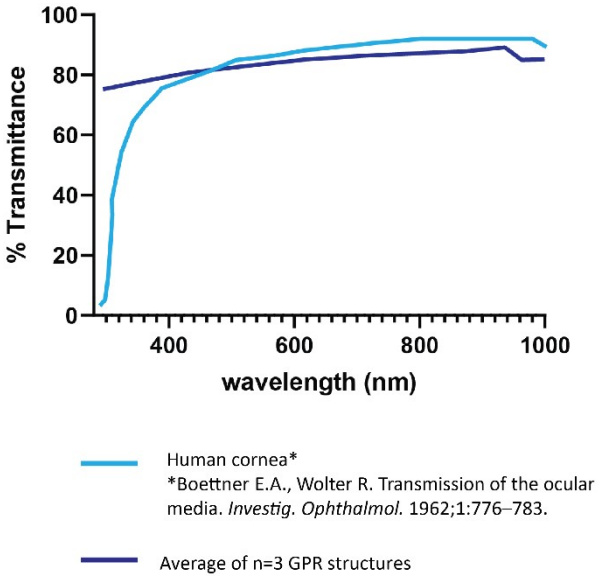

Figure S15. % Transmittance obtained by UV-Vis spectroscopy of the GPR structures after 2 weeks in culture compared to the human cornea.